SHORT COMMUNICATION

Inhibition of temperature-sensitive TRPV3 channel by two natural isochlorogenic acid isomers for alleviation of dermatitis and chronic pruritus

Hang Qi[a], Yuntao Shi[b], Han Wu[a], Canyang Niu[a], Xiaoying Sun[a,c,*], KeWei Wang[a,c,*]

[a]Department of Pharmacology, School of Pharmacy, Qingdao University, Qingdao 266021, China
[b]State Key Laboratory of Natural and Biomimetic Drugs, School of Pharmaceutical Sciences, Peking University, Beijing 100191, China
[c]Institue of Innovative Drugs, Qingdao University, Qingdao 266021, China

Abstract   Genetic gain-of-function mutations of warm temperature-sensitive transient receptor potential vanilloid 3 (TRPV3) channel cause Olmsted syndrome characterized by severe itching and keratoderma, indicating that pharmacological inhibition of TRPV3 may hold promise for therapy of chronic pruritus and skin diseases. However, currently available TRPV3 tool inhibitors are either nonselective or less potent, thus impeding the validation of TRPV3 as therapeutic target. Using whole-cell patch-clamp and single-channel recordings, we report the identification of two natural dicaffeoylquinic acid isomers isochlorogenic acid A (IAA) and isochlorogenic acid B (IAB) that selectively inhibit TRPV3 currents with IC_{50} values of 2.7 ± 1.3 and 0.9 ± 0.3 μmol/L, respectively, and reduce the channel open probability to $3.7 \pm 1.2\%$ and $3.2 \pm 1.1\%$ from $26.9 \pm 5.5\%$, respectively. *In vivo* evaluation confirms that both IAA and IAB significantly reverse the ear swelling of dermatitis and chronic pruritus. Furthermore, the isomer IAB is able to rescue the keratinocyte death induced by TRPV3 agonist carvacrol. Molecular docking combined with site-directed mutations reveals two residues T636 and F666 critical for the binding of the two isomers. Taken together, our identification of isochlorogenic acids A and B that act as specific

TRPV3 channel inhibitors and gating modifiers not only provides an essential pharmacological tool for further investigation of the channel pharmacology and pathology, but also holds developmental potential for treatment of dermatitis and chronic pruritus.

1. Introduction

The warm temperature-sensitive Ca^{2+}-permeable transient receptor potential vanilloid 3 (TRPV3) channel is abundantly expressed in the skin keratinocytes, playing a critical role in skin physiology and pathology[1−4]. In humans, genetic gain-of-function mutations in TRPV3 cause Olmsted syndrome (OS) characterized by palmoplantar and periorificial keratoderma, dermatitis, hair loss and severe itch[5,6], and similar genetic mutations in other thermo-TRPs such as TRPV1 and TRPA1 have not been identified yet in humans[7−9]. In rodents, the gain-of-function mutations of TRPV3 also lead to dermatitis, severe itch and abnormal hair growth[10−12]. Activation of TRPV3 enhances inflammatory and itch responses, and causes release of many proinflammatory factors such as interleukins, TSLP and PGE2 secreted from keratinocytes[13−16]. Conversely, suppression of TRPV3 channel function by knockout attenuates chronic pruritus induced by dry skin[17]. These investigations demonstrate that overactive TRPV3 channel is critical in the pathophysiology and progression of skin-related diseases such as dermatitis and chronic pruritus, indicating that pharmacological inhibition of TRPV3 may serve as a therapeutic strategy for skin diseases.

As a multimodal biosensor, TRPV3 is activated by temperature above 32 °C and exogenous ligands including 2-aminoethoxydiphenyl borate (2-APB), carvacrol, camphor, menthol and thymol[18−20]. TRPV3 is also regulated by various physiological factors such as cations (Ca^{2+}, Mg^{2+}, H^+), endogenous ligand farnesyl pyrophosphate, membrane voltage, and arachidonic acid[21−24]. Conversely, TRPV3 can be inhibited by broad TRP channel antagonists ruthenium red[3] and nonselective antagonists isoprene pyrophosphate[25], and 17(R)-resolvin D1[26]. Recently our group reported that pharmacological inhibition of TRPV3 by a relative specific natural compound forsythoside B can rescue cell death caused by excessive activation TRPV3 and also attenuate pruritus[27]. The therapeutic potential of TRPV3 inhibitors in itch and pain is also recently reported by two independent laboratories[28,29]. However, all of these inhibitors are either nonselective or less potent[27−34], and it is imperative to identify selective and potent TRPV3 inhibitors that can be used either to further understand the channel pharmacology or lead to development potential for novel therapy of dermatitis and chronic pruritus.

We recently reported two dicaffeoylquinic acid isomers isochlorogenic acid A (IAA) and isochlorogenic acid B (IAB) as active ingredients of extracts from a herb *Achillea alpina* that display inhibitory activity on TRPV3 channel[35]. However, whether IAA and IAB can directly target TRPV3 channel or alleviate skin inflammation and pruritus remains unknown. In this study, we investigated the effects of the two isomers IAA and IAB on specific inhibition of TRPV3 and identified two key residues critical for inhibition of the channel. Both IAA and IAB can significantly reverse dermatitis of ear swelling and chronic pruritus. Our findings demonstrate that natural isochlorogenic acids A and B as TRPV3 channel gating modifiers not only provide essential tool molecules for further investigation of the channel pharmacology and channelopathy but also may hold developmental potential for therapy of dermatitis and chronic pruritus.

2. Materials and methods

2.1. Animals

Adult male C57BL/6J (8−10-week-old) mice were purchased from Beijing Vital River Laboratory and housed for at least one week for adaptation to a temperature-controlled animal room (22 ± 2 °C) under a 12 h light/dark cycle, with free access to food and water. All animal tests were approved by the Institutional Animal Care and Use Committee of Qingdao University Health Science Center (Qingdao, China).

2.2. Reagents and compounds

Natural compounds isochlorogenic acids A (MW: 516.45) and B (MW: 516.45) were purchased from Shanghai Tauto Biotech Corporation, Ltd. Compounds 2-aminoethoxydiphenyl borate (2-APB), carvacrol (Car), capsaicin, ruthenium red (RR), GSK1016790A (GSK101) and allyl isothiocyanate (AITC) were purchased from Sigma−Aldrich (St. Louis, MO, USA). All compounds were made as stock solutions before use. For patch-clamp recordings, compounds were diluted in perfusion solution. For cell death assay, compounds were diluted in cell culture medium. For ear swelling and chronic pruritus models, compounds were diluted in solvent (ethanol/olive oil = 4/1, *v/v*).

2.3. Cell culture and transient transfection

Human embryonic kidney (HEK) 293 and human immortalized nontumorigenic keratinocyte (HaCaT) cells were maintained in Dulbecco's modified Eagle's medium (DMEM, Gibco) supplemented with 10% fetal bovine serum at 37 °C with 5% CO_2. HEK293 cells were trypsinized and plated onto glass coverslips 24 h before transfection. 2.5 μg cDNAs of human *TRPV3* (*hTRPV3*, accession number NM_145068.4), *hTRPV1* (accession number NM_080704.3), *hTRPV4* (accession number NM_021625.5), *hTRPA1* (accession number NM_007332.3) and mouse *Trpv3* (*mTrpv3*, accession number AF510316.1) were transiently transfected into cells in a 35-mm cell culture dish with Lipofectamine 2000 (Invitrogen) following the manufacture's protocol. Cells transfected with human *TRPV3* cDNAs were used for determination of cell death and proliferation. *hTRPV3* transfected cells were also used for evaluation of dicaffeoylquinic acid isomers isochlorogenic acid A (IAA) and isochlorogenic acid B (IAB) in whole-cell and single-channel recording assays. Cells transfected with mouse *Trpv3* cDNA or mutant cDNAs were used for identification of residues critical for binding of IAA and IAB. Patch-clamp recordings were carried out 18 h after transfection. Transfected cells were identified with green fluorescence based on

expression of enhanced GFP (EGFP) as an indicator before electrophysiological recordings.

2.4. Electrophysiological recordings

Patch-clamp recordings were performed using an EPC10 amplifier powered by PatchMaster software (HEKA). For whole-cell patch clamp recordings, borosilicate glass pipettes were pulled using a DMZ universal electrode puller (Zeitz-Instruments GmbH) and fire-polished to resistance about ~4.0 MΩ. HEK293 cell was held at 0 mV and current was elicited by 500-ms voltage ramp from −100 to +100 mV with 2 s intervals[27,36]. For inside-out patch recordings of single-channel, pipettes were pulled for a higher resistance of 6−10 MΩ. Membrane potential was held at 0 mV before a testing pulse of +80 mV. Both bath and pipette solutions contained 130 mmol/L NaCl, 0.2 mmol/L EDTA, 3 mmol/L HEPES and 10 mmol/L glucose, pH 7.4 adjusted with NaOH. Single channel currents were sampled at 10 kHz and filtered at 2.9 kHz. All recordings were performed at room temperature (22−24 °C) and data were analyzed with Igor Pro (Wave-metrics) and Origin 8.6 (OriginLab).

2.5. Molecular docking and site-directed mutagenesis

Molecular docking was performed using Schrödinger Glide (Maestro software suite 2015, Schrödinger, New York, USA). Small molecules IAA and IAB were drawn using ChemBioDraw Ultra 14.0 (CambridgeSoft) and optimized for docking using a built-in program Ligprep in Maestro. The mTRPV3 EM structure was obtained from Protein Data Bank (PBD code: 6DVW) and prepared for the docking following the standard procedure of Maestro using the standard docking module SP. The binding pocket of ligand with mTRPV3 was selected based on the reported inhibitor binding sites of TRPV3, TRPV1[37] and TRPA1[38], using Glide and ranked by the resulting score. The pore helix and S6 of the mTRPV3 were chosen to be the binding pocket for IAA and IAB based on its highest ranking. All mTRPV3 site-directed mutations were generated with Mut Express II Fast Mutagenesis Kit following the manufacture's instructions. All mutants were confirmed by sequencing for correct generation of mutagenesis.

2.6. Cell death assay

HEK293 cells transfected with *hTRPV3* cDNA post 12 h or HaCaT cells were equally seeded in six-well culture plates and randomly divided into 6 groups. Treatment with different compounds for 12 h, HEK293 and HaCaT cells were treated with 0.25% trypsin (Gibco) for 1 and 7 min, respectively. After centrifugation, cells were resuspended with PBS buffer containing Hoechst and propidium iodide (PI) for 30 min. Five random view images were taken under a microscope (Eclipse Ti; Nikon) for each group and automatically counted on a confocal microscope (A1R MP; Nikon). The cell death ratio was defined as an average dead cells (PI-labeled nuclei) over total cells (Hoechst-labeled nuclei) from five images[27].

2.7. Cell proliferation assay

HEK293 cells transfected with *hTRPV3* channel or HaCaT cells (5×10^3 per well) were seeded in 96-well plates for 24 h before exposed to TRPV3 activator or inhibitor for another 24 h. The cell viability was assessed by adding 20 μL of tetrazolium salt MTT (5 mg/mL, Sigma−Aldrich) to each well for 4 h before removal of the culture medium for measurement of reductive product formazan dissolved in 150 μL DMSO under the light absorbance at 490 nm in a Sunrise microplate reader (TECAN, Swissland)[39].

2.8. Generation of ear swelling and chronic pruritus models induced by TRPV3 agonist carvacrol

For induction of mouse ear swelling, 3% carvacrol (carvacrol/solvent = 3/97, *v/v*) was dissolved in solvent (ethanol/olive oil = 4/1, *v/v*) and topically applied once a day onto the right ear for 6 consecutive days[40]. Compounds IAA and IAB (1.0 mmol/L in 50 μL) were dissolved in the solvent (ethanol/olive oil = 4/1, *v/v*) and applied onto the same ear 30 min after the application of 3% carvacrol for 6 consecutive days. Solvent (ethanol/olive oil = 4/1, *v/v*) contained 1% DMSO was used as vehicle control. Ear thickness was first measured 30 min before initial application of 3% carvacrol and continued to measure for 7 consecutive days with a Vernier caliper (7D-01150, FORGESTAR) at an accuracy of 0.02 mm. Scratching behavior was recorded for 1 h on the day 7 as previously described[27,41].

2.9. Statistical analysis

All data are expressed as the mean ± standard error of mean (SEM). Statistical significance was assessed by unpaired *t* test, one-way analysis of variance (ANOVA) followed by Dunnet's test or two-way ANOVA followed by Bonferroni's multiple comparisons test using GraphPad Prism 7.0 software. A value of $P < 0.05$ is considered to be statistically significant.

3. Results

3.1. Identification of natural dicaffeoylquinic acid isomers IAA and IAB as potent TRPV3 inhibitors

We started performing the whole-cell patch-clamp recordings of hTRPV3 currents expressed in HEK293 cells and individually tested the effects of two natural dicaffeoylquinic acid isomers IAA and IAB at single concentration (50 μmol/L) on hTRPV3 current. Perfusion of IAA or IAB at 50 μmol/L significantly inhibited the channel current activated by agonist 2-APB (50 μmol/L) about 80.8 ± 2.1% (n = 5) and 86.4 ± 3.3% (n = 5), respectively (Fig. 1A and B). Adding different concentrations of either IAA or IAB caused a dose-dependent inhibition of hTRPV3 currents evoked by 2-APB (50 μmol/L) with an IC$_{50}$ value of 2.7 ± 1.3 μmol/L and 0.9 ± 0.3 μmol/L and a Hill coefficient of 0.50 and 0.53, respectively (Fig. 1C and D). These results indicate that both IAA and IAB inhibit hTRPV3 currents in dose-dependent manner with IAB exhibiting a 3-fold better potency.

3.2. Selective inhibition of TRPV3 channel by IAA and IAB

To test the selectivity of IAA and IAB over other thermo-TRP channels previously reported for their involvement in pruritus and inflammation[8,42,43], we recorded the whole-cell currents of TRPV1, TRPV4, and TRPA1 channels expressed in HEK293 cells. Perfusion of IAA or IAB at 50 μmol/L had no obvious inhibition of TRPV1 currents induced by capsaicin (1 μmol/L, Fig. 2A, D and E). Similarly, IAA or IAB (50 μmol/L) had no inhibitory effect on either TRPV4 current elicited by 100 nmol/L GSK1016790A (GSK101, Fig. 2B, D and E) or TRPA1 current evoked by allyl isothiocyanate (AITC) at 300 μmol/L, as compared with TRPV3 current reduction by IAA or IAB (Fig. 2C–E). These results demonstrate that IAA and IAB are selective inhibitors of TRPV3 channels over the tested thermo-TRP channels.

3.3. Direct targeting of TRPV3 single channel by IAA and IAB

To further confirm whether IAA and IAB could directly target single TRPV3 channel, we performed the single-channel recordings of HEK293 cells overexpressing hTRPV3 in an inside-out patch configuration. As control, application of TRPV3 activator carvacrol (300 μmol/L) increased the channel opening from open level 1 (O1) to level 2 (O2) with single channel conductance of 168.4 ± 2.1 pS and channel open probability about 90-fold to $26.9 \pm 5.5\%$ from $0.3 \pm 0.2\%$ as vehicle control (Fig. 3A, B, F and G). Adding IAA or IAB at 100 μmol/L in the presence of carvacrol (300 μmol/L) resulted in a significant reduction of the channel open probability to $3.7 \pm 1.2\%$ ($n = 4$, $P < 0.0001$) and $3.2 \pm 1.1\%$ ($n = 4$, $P < 0.0001$), respectively (Fig. 3C, D and G). We also tested the inhibition of TRPV3 activation by a non-
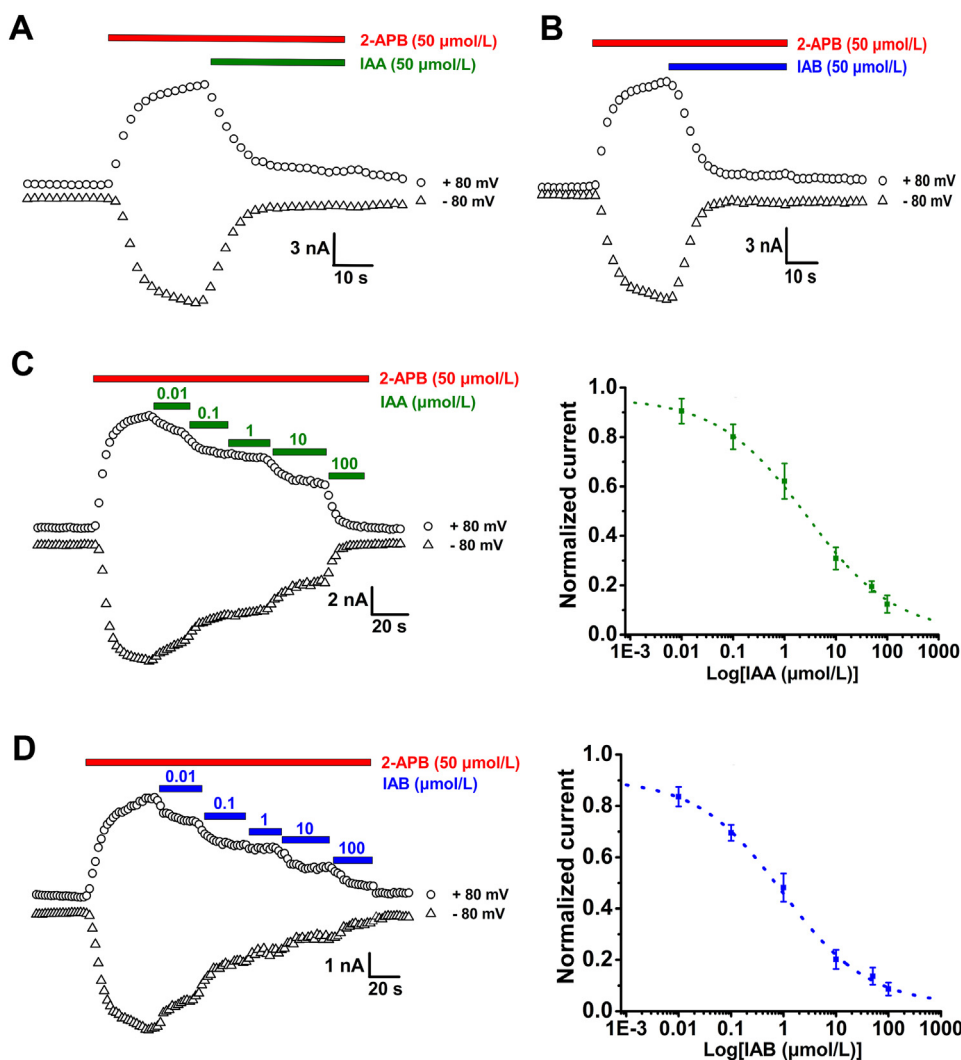

Figure 1 Concentration-dependent inhibition of whole-cell hTRPV3 currents expressed in HEK293 cells by natural IAA and IAB. hTRPV3 currents activated by 50 μmol/L 2-APB were inhibited by IAA (A) or IAB (B) at 50 μmol/L in the presence of 2-APB ($n = 5$). (C) Inhibition of whole-cell currents by increasing concentrations of IAA at 0.01–100 μmol/L (left panel) and analysis of concentration-dependent inhibition of hTRPV3 outward currents at +80 mV by IAA with fitting to a Hill equation, with an IC$_{50}$ value of 2.7 ± 1.3 μmol/L ($n = 5$–6) (right panel). (D) Left panel, whole-cell hTRPV3 currents in response to increasing concentrations of IAB (0.01–100 μmol/L). Right panel, dose-response relationships of hTRPV3 outward currents at +80 mV inhibited by IAB with fitting to a Hill equation, with an IC$_{50}$ value of 0.9 ± 0.3 μmol/L ($n = 6$–8). Whole-cell currents were evoked by voltage ramps from −100 mV to +100 mV for duration of 500 ms. Data are shown as the mean $\pm$ SEM.

selective TRP channel pore blocker ruthenium red (RR, 20 μmol/L) that also reduced the single channel open probability to $0.5 \pm 0.4\%$ from $26.9 \pm 5.5\%$ and single-channel conductance to 122.8 ± 5.5 pS from 175.2 ± 0.9 pS ($n = 4$, $P < 0.0001$; Fig. 3E–G). These results confirm the direct inhibition of single TRPV3 channel by either IAA or IAB.

3.4. Reversal of ear swelling and chronic pruritus by topical treatment of IAA and IAB

Overactive TRPV3 causes severe itch and cutaneous inflammation in both rodents and humans[5,11,44,45]. To mimic TRPV3 channelopathy, we carried out topical application of carvacrol (3%) in mouse right ear for 6 consecutive days and generated the model of
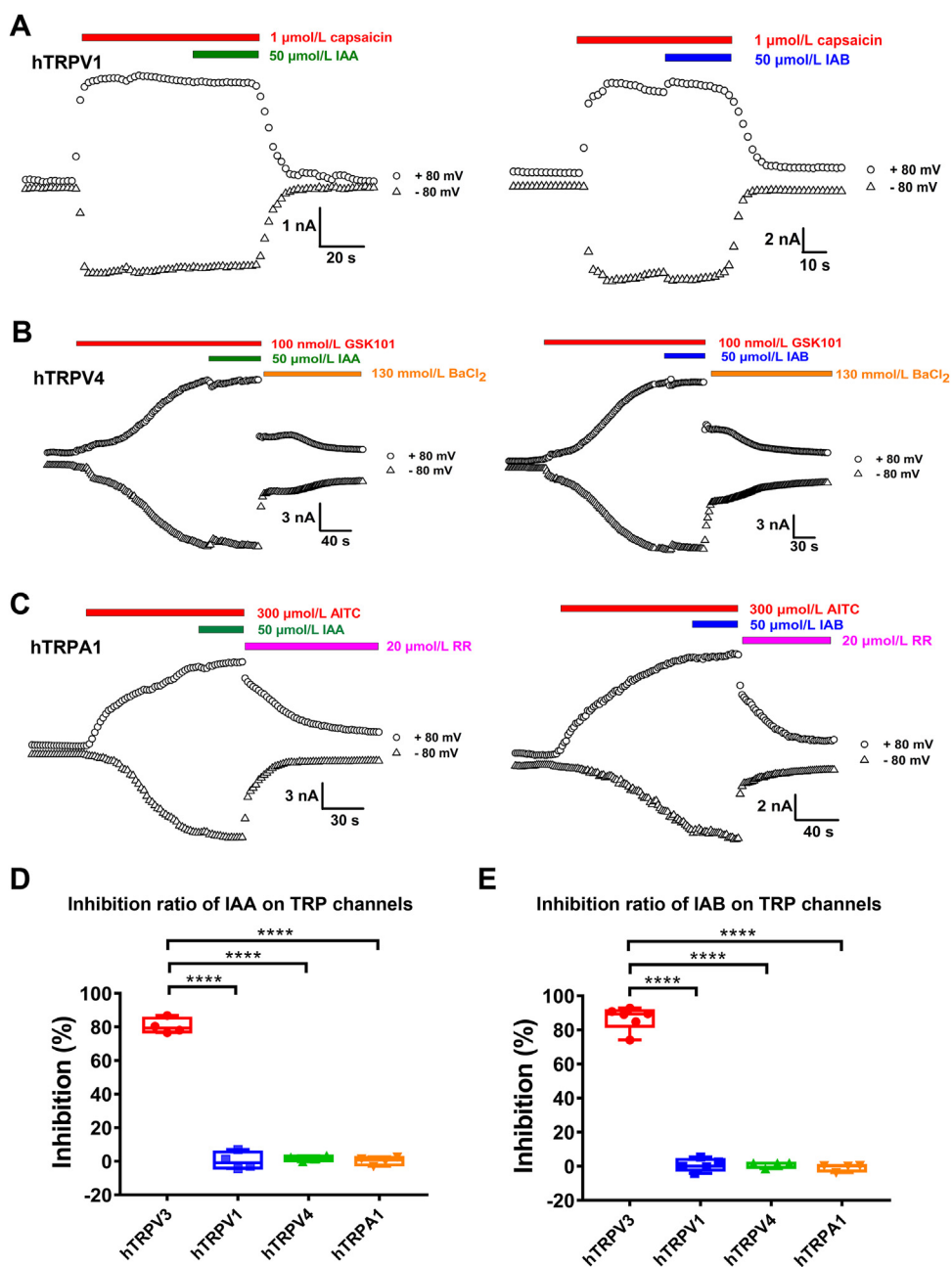
Figure 2 Selective inhibition of whole-cell TRPV3 currents by IAA and IAB over other thermoTRP channels transiently expressed in HEK293 cells. (A) Whole-cell current of TRPV1 in response to 1 μmol/L capsaicin, and co-application of 50 μmol/L IAA (left panel) or IAB (right panel) displaying no inhibition on TRPV1. (B) TRPV4 current evoked by 100 nmol/L GSK1016790A (GSK101) or inhibited by 130 mmol/L $BaCl_2$, in comparison with co-application of 50 μmol/L IAA (left panel) or IAB (right panel) that had no inhibitory effect. (C) TRPA1 current was activated by 300 μmol/L allyl isothiocyanate (AITC), and co-application of 50 μmol/L IAA (left panel) or IAB (right panel), and inhibited by 20 μmol/L ruthenium red (RR). (D) Summary for average current inhibition of hTRPV3, hTRPV1, hTRPV4, and hTRPA1 channels by 50 μmol/L IAA. (E) Summary for average current inhibition of hTRPV3, hTRPV1, hTRPV4, and hTRPA1 channels by 50 μmol/L IAB. Data are shown as the mean $\pm$ SEM, $n = 4$–6; ****$P < 0.0001$, by unpaired t test.
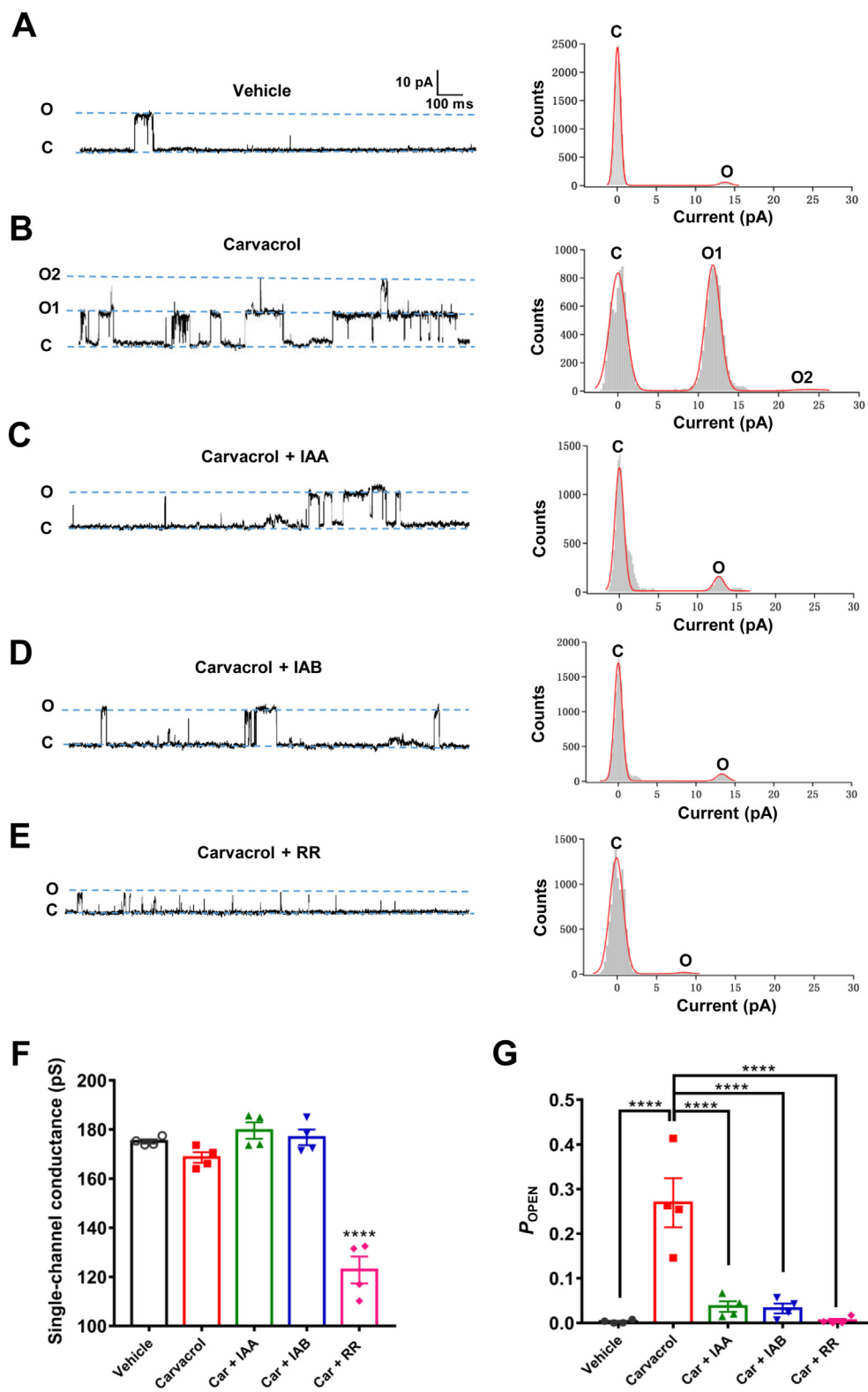
Figure 3 Reduction of single hTRPV3 channel open probability by IAA and IAB. (A)−(E) Left panels, representative traces recorded from an inside-out patch in the condition of vehicle (A), after addition of 300 μmol/L carvacrol (B), co-perfusion of 100 μmol/L IAA and 300 μmol/L carvacrol (C), co-perfusion of 100 μmol/L IAB and 300 μmol/L carvacrol (D), and co-perfusion of 20 μmol/L RR and 300 μmol/L carvacrol (E). Right panels, all-points histograms of single-channel current recording data as shown in left panels and their histograms were fitted to a Gauss functions. (F) Summary of hTRPV3 single channel conductance after exposure to different regulators (Car: carvacrol; RR: ruthenium red. $n = 4$, ****$P < 0.0001$, compared with vehicle control). (G) Summary for calculated single hTRPV3 channel mean P_{OPEN} values in the presence of different TRPV3 modulators ($n = 4$, ****$P < 0.0001$). Data are shown as the mean ± SEM; ****$P < 0.0001$, by one-way ANOVA, followed by the Dunnet's test.
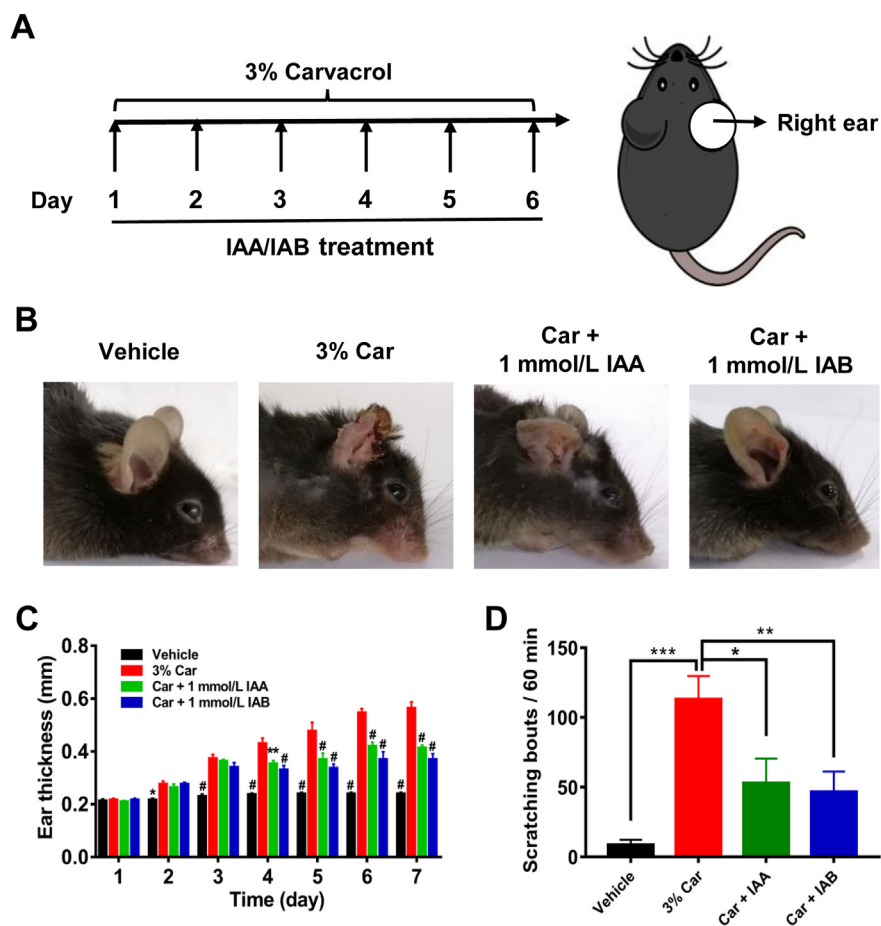
Figure 4 IAA and IAB attenuates ear swelling and scratching behavior. (A) Schematic diagram of experimental timeline and location for generation of chronic itch and ear swelling model. (B) Representative ear appearance in wild type mice topically applied with vehicle, carvacrol (Car), IAA and IAB for 6 consecutive days. (C) Summary for right ear thickness from groups of vehicle, carvacrol, IAA and IAB for 7 consecutive days ($n = 6$ mice for per group, **$P < 0.01$, #$P < 0.001$, compared with carvacrol-treated group, by two-way ANOVA, followed by the Bonferroni's test). (D) Summary for spontaneous right ear scratching bouts with or without compound treatment on the Day 7 ($n = 6-8$ mice per group, *$P < 0.05$, **$P < 0.01$, ***$P < 0.001$ by one-way ANOVA, followed by the Dunnet's test). Data are presented as the mean $\pm$ SEM.

chronic dermatitis characterized by swelling and dermatitis (Fig. 4A and B). Topical treatment of either IAA or IAB (1 mmol/L) for four days showed obvious attenuation of epidermal inflammation and ear swelling in mouse right ears ($n = 6$, $P < 0.05$; Fig. 4B and C), as compared to mice only treated with 3% carvacrol. Similarly, application of IAA and IAB (1 mmol/L) also reduced the number of scratching bouts to 52.9 ± 17.7 ($n = 8$, $P < 0.05$) and 46.6 ± 14.5 ($n = 8$, $P < 0.01$) from 113.0 ± 16.9, respectively (Fig. 4D). These results demonstrate that selective inhibition of TRPV3 by either IAA or IAB can attenuate dermatitis and chronic pruritus.

3.5. IAB rescues HEK293 and HaCaT cell death induced by excessive activation of TRPV3

Genetic or pharmacological activation of TRPV3 causes keratinocyte cell death[5,14]. To examine whether TRPV3 inhibition could rescue the cell death induced by overactive TRPV3 function, we evaluated the effect of IAB on cell death caused by TRPV3 channel agonist carvacrol in both hTRPV3 expressed HEK293 cells and HaCaT cells. As shown in Fig. 5A and B,

HEK293 cells expressing TRPV3 treated with carvacrol (300 μmol/L) for 12 h exhibited an increased ratio of cell death to $21.1 \pm 1.9\%$ ($n = 4$, $P < 0.0001$), compared with vehicle at $5.3 \pm 0.5\%$ ($n = 4$). In contrast, application of 10 and 100 μmol/L IAB decreased the cell death ratio to $11.7 \pm 0.9\%$ ($n = 4$, $P < 0.001$) and $9.9 \pm 1.2\%$ ($n = 4$, $P < 0.0001$), respectively. As a positive control, ruthenium red also reduced the cell death ratio to $14.3 \pm 1.7\%$ ($n = 4$, $P < 0.01$). In HaCaT cells, TRPV3 activation by 300 μmol/L carvacrol for 12 h also led to an elevated cell death ratio of $13.0 \pm 2.1\%$ (Fig. 5C and D). Similarly, adding IAB resulted in a dose-dependent reduction of HaCaT cell death. These data show that inhibition of TRPV3 activity rescues cell death induced by the channel activation.

We also tested the effect of IAB on cell proliferation using an MTT assay. Activation of TRPV3 by carvacrol (300 μmol/L) suppressed the cell proliferation of hTRPV3-HEK293 cells or HaCaT cells (Supporting Information Fig. S1). In contrast, IAB at 10 and 100 μmol/L significantly reversed overactive TRPV3-induced inhibition of cell proliferation (Fig. S1). These results further demonstrate that IAB can attenuate overactive TRPV3-induced inhibition of cell proliferation.

3.6. Identification of TRPV3 channel residues critical for IAA and IAB binding by molecular docking and site-directed mutagenesis

To further identify residues critical for IAA and IAB binding to TRPV3, we carried out the molecular docking of IAA and IAB onto the cryo-EM structure of mouse TRPV3 (PDB: 6DVW) using the Glide model of Schrödinger[46]. The docking analysis reveals that both IAA and IAB are confined in the central cavity pocket near the pore helix and S6 segment, with their binding scores of −8.9 and −9.1, respectively (Fig. 6A and B). Upon its binding, IAA is recognized by residues L635, T636, V662, F666 and L669 through several van der Waals forces (light blue dotted lines) and residue L635 through one hydrogen bond (Fig. 6C, orange dotted line). In a different interaction as compared to IAA, IAB binds to three residues F590, F666 and L669 through van der Waals forces, and also one T665 residue and two T636 residues from neighboring two subunits through four hydrogen bonds (Fig. 6D), thus forming a "clamp-like" interaction. Such a "clamp-like" fashion indicates a tighter fit for IAB that is more potent than its isomer IAA.

To further confirm the key binding residues from the docking, we made alanine mutations for six residues L635A, T636A, V662A, T665A, F666A and L669A that are critical for the formation of the central cavity pocket and are also conserved between species of mouse TRPV3 and human TRPV3 (Supporting Information Fig. S2). Patch-clamp recordings confirmed that mutating two residues T636 and F666 markedly reduced IAA- or IAB-induced inhibition of mTRPV3 currents (Fig. 6G−I), as compared with WT mTRPV3 (Fig. 6E and F), while mutating three residues V662, T665 and L669 had no obvious effect on IAA- or IAB-induced inhibition of mTRPV3 currents (Fig. 6I). We were unable to test the effect of IAA or IAB on L635A mutant that was insensitive to TRPV3 activation by 2-APB (50 μmol/L), likely due to the mutant affecting its surface expression[29,46]. All together, these results demonstrate that two residues T636 in the pore helix and F666 in the S6 segment are critical for forming noncovalent interactions with IAA and IAB and mediating the channel inhibition.

We also docked IAA and IAB into other two pockets such as the capsaicin binding site in TRPV1 (orange mesh, Supporting Information Fig. S3) and 2-APB binding site in TRPV3 (purple mesh, Fig. S3)[37,46−48]. The docking scores for capsaicin and 2-APB sites are much lower than that in the central cavity pocket (Supporting Information Table S1), suggesting that IAA and IAB are less likely to bind to these two sites.

We further examined if IAA and IAB could function as competitive antagonists to bind to the known 2-APB pocket for competition with 2-APB for the same residue[35]. Mutating the residue H426 critical for 2-APB binding to mTRPV3 into alanine resulted in the channel mutant (H426A) that was not activated by 2-APB (50 μmol/L). In contrast, mTRPV3 H426A mutant current was activated by specific agonist carvacrol (Supporting Information Fig. S4A) and the carvacrol-mediated H426A mutant currents were markedly inhibited by IAA or IAB (Fig. S4B−S4F). These results suggest that the isomers are unlikely to bind to the residue H426 that is critical for 2-APB and are less likely confined in the 2-APB pocket.
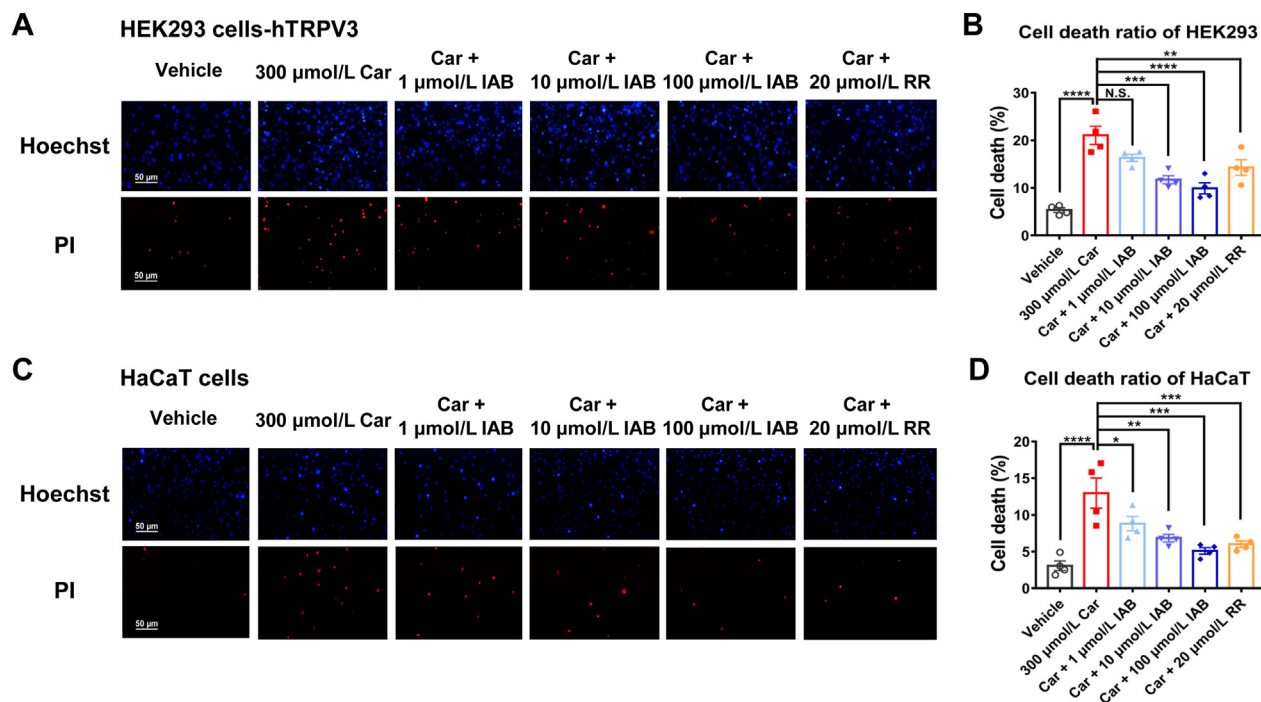
Figure 5 IAB attenuates cell death of HEK293 cells expressing hTRPV3 and HaCaT cells. (A) Representative images of Hoechst staining labeled for cell nuclei (top panels) and PI staining labeled for dead cells (bottom panels) from TRPV3-expressed HEK293 cells treated with different compounds for 12 h. Scale bar, 50 μm. (B) Summary for cell death ratio from (A). (C) Representative images of Hoechst staining (top panels) and PI staining (bottom panels) of HaCaT cells treated with different compounds for 12 h. (D) Summary for cell death ratio from (C). Data are shown as the mean ± SEM, n = 4, *P < 0.05, **P < 0.01, ***P < 0.001, ****P < 0.0001, N.S., no significance, by one-way ANOVA, followed by the Dunnet's test.
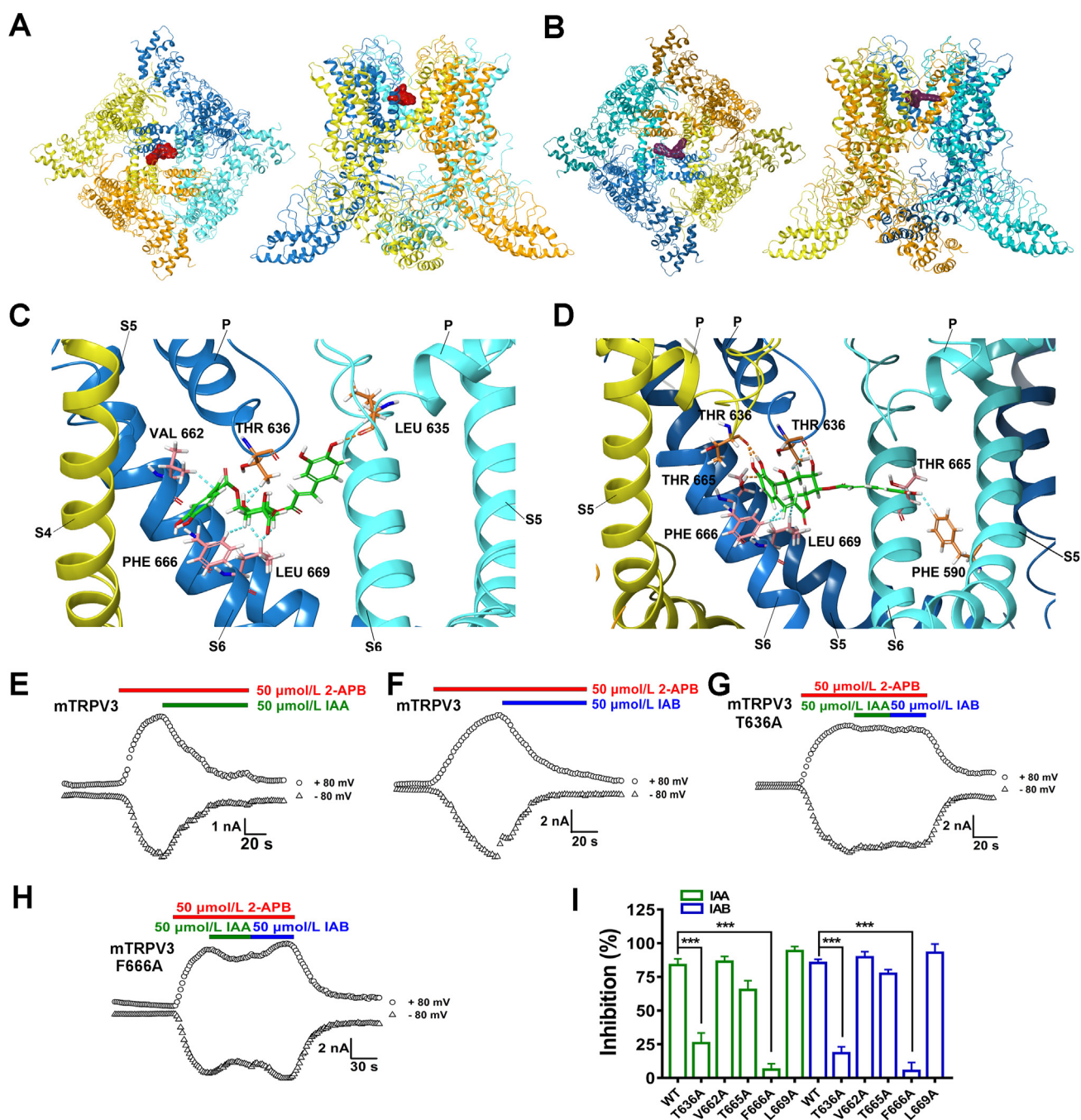
Figure 6 Critical binding sites for gating modifiers IAA and IAB in mouse TRPV3 channel. Representative bound conformations of IAA (A) and IAB (B) confined to the pocket consisting of the pore helix and S6 segment in top-down view (left panel) and side view (right panel). IAA and IAB are shown in red and purple surfaces, respectively. Side view of IAA (green) and TRPV3 subunit interactions (C), and IAB (green) and TRPV3 subunit interactions (D). Hydrogen bonds and van der Waals forces are shown as orange and light blue dotted lines, respectively. Three TRPV3 subunits are shown in blue, cyan and yellow. Representative current traces of wild type mTRPV3 (E and F), T636A (G) and F666A (H) mutants expressed in HEK293 cells in responses to 2-APB alone and 2-APB with IAA or IAB. (I) Summary for WT mTRPV3 or mutant channel current inhibition by 50 μmol/L IAA and IAB ($n = 3-8$). Data are shown as the mean ± SEM, ***$P < 0.001$, by unpaired t test.

4. Discussion

Identification of small molecule tools specifically targeting TRPV3 is necessary for validation of the channel as therapeutic target and potential therapy. In this study, we identified two natural isomers of isochlorogenic acids A and B that selectively inhibit TRPV3 channels and alleviate dermatitis and chronic pruritus.

Molecular docking combined with site-directed mutagenesis further reveals residues critical for their interactions between the isomers and TRPV3 channel. Our identification of isochlorogenic acids A and B not only reveals a mechanistic explanation for their anti-inflammation, but also provides pharmacological tools for validation of TRPV3 channel target and developmental potential for therapy of skin diseases.

Isochlorogenic acids A and B are regioisomers of each other and are active ingredients of *A. alpina* and *Laggera alata* plants, mainly distributed in eastern and southeastern Asia[35,49,50]. *A. alpina* and *L. alata* rich in dicaffeoylquinic acid derivatives are traditionally used as medicinal herbs, especially for treatment of inflammation-related diseases[35,51,52]. Polyphenols extracts from kuding tea plant containing isochlorogenic acids A and B can reduce the release of TNF-α, IL-6 and IL-1β in mice with UVB-induced skin inflammation[53]. Isochlorogenic acids A and B also have been shown to exhibit anti-inflammatory activities by inhibiting NF-κB signaling pathway[50,52] and to suppresses oxidant stress, pulmonary edema, cell apoptosis and inflammatory factors[54,55]. In this study, our findings reveal a novel molecular mechanism of action for isochlorogenic acids A and B that directly target and inhibit temperature-sensitive TRPV3 channel that plays critical role in skin physiology and pathology.

Dermatitis and pruritus are common symptoms of chronic cutaneous diseases that present a highly unmet clinical needs[56,57]. Emerging evidence reveals that TRP channels are critically involved in regulating various cutaneous functions both in physiological and pathophysiological conditions[7,58]. For example, TRPV1 is able to mediate histamine induced itch[59]. TRPA1 is required for mediating no-histaminergic pruritogens such as CQ, BAM8-22, SLIGRL and TSLP evoked itch[42,60]. TRPV1 and TRPA1 are also involved in inflammation related dermatitis[42,61]. TRPV3 as a cutaneous biosensor plays a crucial role in skin physiology and pathology[3,18,62]. The ultimate proof for TRPV3 as a potential target on cutaneous disease based on the identification of gain-of-function site mutations of TRPV3 in rodent that cause dermatitis and in human that cause OS[5,11,44]. In this study, in order to validate TRPV3 as a promising target for chronic pruritus and dermatitis treatment, we generated a chronic pruritic and inflammatory models by pharmacological activation of TRPV3 with 3% carvacrol. IAA and IAB treated mice displayed alleviative hyperkeratosis and scarring in the epidermis of right ears (Fig. 4B), alleviative ear swelling (Fig. 4C) and reduced number of scratching bouts (Fig. 4D), suggesting that pharmacological inhibition of TRPV3 by IAA and IAB may hold developmental potential for therapy of chronic pruritus and dermatitis. A recent report shows that a TRPV3 inhibitor 74a also can attenuate scratching and dermatitis symptoms in a mouse model of atopic dermatitis[9], although its selectivity over other thermo-TRPs such as TRPV4 and TRPA1 remains to be further confirmed[33]. OS patients also characterized by diffuse palmoplantar and periorificial keratoderma may impute to the overactive TRPV3 of keratinocytes, that causes calcium overload resulting in keratinocyte cell death and keratinization[5,21], that's consistent with our results and IAB is able to rescue the HaCaT cell death by inhibiting the overactive TRPV3 (Fig. 5). It has been shown that both TRPV1 and TRPV3 channels can coassemble to form functional channels[63,64]. Therefore, it is possible that pharmacological inhibition of either TRPV3 or TRPV1 may lead to synergistic suppression of their heteromeric channel function, and dual inhibition of TRPV1 and TRPV3 may present the best therapeutic potential for skin diseases in clinical practice.

Both IAA and IAB likely act as the gating modifiers of TRPV3 channel by interacting with the key residue F666, and we guess the interaction may cause the S6 helix undergoing a transition to a closed conformation (α-helix) from an opening state (π-helix) according to the observation that TRPV3 channel opening results from each S6 helix undergoing a local α-to-π helical transition that begins at residue F666 and results in an outward expansion

about 11° away from the pore[46,65]. Our mutagenesis and functional recording results also suggested that IAA and IAB are confined in the central cavity pocket but not in the previously putative 2-APB pocket[35]. At single-channel level, IAA and IAB exhibit no effect on ion permeation or alteration of the single-channel conductance (Figs. 3 and 6). The mechanism of action of the two isomers is in contrast to channel blocker ruthenium red (RR) that inhibits TRPV3 single-channel conductance by binding to the aspartic acid D641, a key negatively charged acidic residues in the selective filter[66−68].

Our molecular docking and mutagenesis analyses suggest that IAB exhibits about three-fold better potency than IAA that primarily binds to the L635 residue through formation of one hydrogen bond within the central cavity pocket. In contrast, IAB appears to bind to two T636 residues from neighboring two subunits and one T665 residue through formation of four hydrogen bonds in a "clamp-like" fashion (Fig. 6C and D), thus forming a more stable interaction. Such a "clamp-like" interaction for IAB may explain its enhanced potency and serve as a strategy for further improvement by chemical modifications of IAA/IAB for their derivatives. For instance, the hydroxyl group of pyrocatechol and cyclohexane as hydrogen bond donor can be replaced by amidogen or carboxyl groups in order to increase hydrogen bonds interactions between TRPV3 cavity pocket and isochlorogenic acid derivatives. In addition, whether isochlorogenic acid has multi-chiral center essential for potent inhibition of TPRV3 also remains worthy of further investigations.

5. Conclusions

We identified two natural isomers of isochlorogenic acids IAA and IAB that act as TRPV3 channel gating modifiers and selectively inhibited the channel currents by reducing the channel open probability. Both IAA and IAB attenuated keratinocyte cell death, ear swelling and chronic pruritus induced by overactive TRPV3. Molecular docking combined with site-directed mutations revealed two residues T636 and F666 critical for the interaction between the isomers and TRPV3, with IAB forming a clamp-like interaction for enhanced potency of TRPV3 inhibition. Therefore, IAA and IAB not only may be beneficial for the therapy of keratinocytes death related keratoderma, dermatitis and chronic pruritus, but also can provide essential pharmacological tools for further investigating the channel pharmacology and pathology.

Author contributions

Hang Qi, Xiaoying Sun and KeWei Wang designed the project; Hang Qi, Yuntao Shi and Han Wu performed the project; Hang Qi, Hang Wu and Canyang Niu analyzed the data; Hang Qi, Xiaoying Sun and KeWei Wang wrote the manuscript.

Conflicts of interest

The authors declare no conflicts of interest.

Appendix A. Supporting information

Supporting data to this article can be found online at https://doi.org/10.1016/j.apsb.2021.08.002.

References

1. Xu H, Ramsey IS, Kotecha SA, Moran MM, Chong JA, Lawson D, et al. TRPV3 is a calcium-permeable temperature-sensitive cation channel. *Nature* 2002;**418**:181−6.
2. Smith GD, Gunthorpe MJ, Kelsell RE, Hayes PD, Reilly P, Facer P, et al. TRPV3 is a temperature-sensitive vanilloid receptor-like protein. *Nature* 2002;**418**:186−90.
3. Luo J, Hu H. Thermally activated TRPV3 channels. *Curr Top Membr* 2014;**74**:325−64.
4. Cheng X, Jin J, Hu L, Shen D, Dong XP, Samie MA, et al. TRP channel regulates EGFR signaling in hair morphogenesis and skin barrier formation. *Cell* 2010;**141**:331−43.
5. Lin Z, Chen Q, Lee M, Cao X, Zhang J, Ma D, et al. Exome sequencing reveals mutations in TRPV3 as a cause of Olmsted syndrome. *Am J Hum Genet* 2012;**90**:558−64.
6. Duchatelet S, Hovnanian A. Olmsted syndrome: clinical, molecular and therapeutic aspects. *Orphanet J Rare Dis* 2015;**10**:33.
7. Tóth BI, Oláh A, Szöllősi AG, Bíró T. TRP channels in the skin. *Br J Pharmacol* 2014;**171**:2568−81.
8. Dong X, Dong X. Peripheral and central mechanisms of itch. *Neuron* 2018;**98**:482−94.
9. Zhao J, Munanairi A, Liu XY, Zhang J, Hu L, Hu M, et al. PAR2 mediates itch *via* TRPV3 signaling in keratinocytes. *J Invest Dermatol* 2020;**140**:1524−32.
10. Asakawa M, Yoshioka T, Matsutani T, Hikita I, Suzuki M, Oshima I, et al. Association of a mutation in TRPV3 with defective hair growth in rodents. *J Invest Dermatol* 2006;**126**:2664−72.
11. Yoshioka T, Imura K, Asakawa M, Suzuki M, Oshima I, Hirasawa T, et al. Impact of the Gly573Ser substitution in TRPV3 on the development of allergic and pruritic dermatitis in mice. *J Invest Dermatol* 2009;**129**:714−22.
12. Yoshioka T, Hikita I, Asakawa M, Hirasawa T, Deguchi M, Matsutani T, et al. Spontaneous scratching behaviour in DS-Nh mice as a possible model for pruritus in atopic dermatitis. *Immunology* 2006;**118**:293−301.
13. Sun X, Qi H, Wu H, Qu Y, Wang K. Anti-pruritic and anti-inflammatory effects of natural verbascoside through selective inhibition of temperature-sensitive Ca^{2+}-permeable TRPV3 channel. *J Dermatol Sci* 2020;**97**:229−31.
14. Szollosi AG, Vasas N, Angyal A, Kistamas K, Nanasi PP, Mihaly J, et al. Activation of TRPV3 regulates inflammatory actions of human epidermal keratinocytes. *J Invest Dermatol* 2018;**138**:365−74.
15. Park CW, Kim HJ, Choi YW, Chung BY, Woo SY, Song DK, et al. TRPV3 channel in keratinocytes in scars with post-burn pruritus. *Int J Mol Sci* 2017;**18**:2425.
16. Huang SM, Lee H, Chung MK, Park U, Yu YY, Bradshaw HB, et al. Overexpressed transient receptor potential vanilloid 3 ion channels in skin keratinocytes modulate pain sensitivity *via* prostaglandin E2. *J Neurosci* 2008;**28**:13727−37.
17. Yamamoto-Kasai E, Imura K, Yasui K, Shichijou M, Oshima I, Hirasawa T, et al. TRPV3 as a therapeutic target for itch. *J Invest Dermatol* 2012;**132**:2109−12.
18. Wang G, Wang K. The Ca^{2+}-permeable cation transient potential TRPV3 channel: an emerging pivotal target for itch and skin diseases. *Mol Pharmacol* 2017;**92**:193−200.
19. Xu H, Delling M, Jun JC, Clapham DE. Oregano, thyme and clove-derived flavors and skin sensitizers activate specific TRP channels. *Nat Neurosci* 2006;**9**:628−35.
20. Hu H, Grandl J, Bandell M, Petrus M, Patapoutian A. Two amino acid residues determine 2-APB sensitivity of the ion channels TRPV3 and TRPV4. *Proc Natl Acad Sci U S A* 2009;**106**:1626−31.
21. Cao X, Yang F, Zheng J, Wang K. Intracellular proton-mediated activation of TRPV3 channels accounts for the exfoliation effect of alpha-hydroxyl acids on keratinocytes. *J Biol Chem* 2012;**287**:25905−16.
22. Bang S, Yoo S, Yang TJ, Cho H, Hwang SW. Farnesyl pyrophosphate is a novel pain-producing molecule *via* specific activation of TRPV3. *J Biol Chem* 2010;**285**:19362−71.
23. Nilius B, Biro T, Owsianik G. TRPV3: time to decipher a poorly understood family member!. *J Physiol* 2014;**592**:295−304.
24. Liu J, Wang Y, Lin L. Small molecules for fat combustion: targeting obesity. *Acta Pharm Sin B* 2019;**9**:220−36.
25. Bang S, Yoo S, Yang TJ, Cho H, Hwang SW. Isopentenyl pyrophosphate is a novel antinociceptive substance that inhibits TRPV3 and TRPA1 ion channels. *Pain* 2011;**152**:1156−64.
26. Bang S, Yoo S, Yang TJ, Cho H, Hwang SW. 17(R)-Resolvin D1 specifically inhibits transient receptor potential ion channel vanilloid 3 leading to peripheral antinociception. *Br J Pharmacol* 2012;**165**:683−92.
27. Zhang H, Sun X, Qi H, Ma Q, Zhou Q, Wang W, et al. Pharmacological inhibition of the temperature-sensitive and Ca^{2+}-permeable transient receptor potential vanilloid TRPV3 channel by natural forsythoside B attenuates pruritus and cytotoxicity of keratinocytes. *J Pharmacol Exp Ther* 2019;**368**:21−31.
28. Han Y, Luo A, Kamau PM, Takomthong P, Hu J, Boonyarat C, et al. A plant-derived TRPV3 inhibitor suppresses pain and itch. *Br J Pharmacol* 2021;**178**:1669−83.
29. Liu Q, Wang J, Wei X, Hu J, Ping C, Gao Y, et al. Therapeutic inhibition of keratinocyte TRPV3 sensory channel by local anesthetic dyclonine. *ELife* 2021;**10**:e68128.
30. Bischof M, Olthoff S, Glas C, Thorn-Seshold O, Schaefer M, Hill K. TRPV3 endogenously expressed in murine colonic epithelial cells is inhibited by the novel TRPV3 blocker 26E01. *Cell Calcium* 2020;**92**:102310.
31. Sun XY, Sun LL, Qi H, Gao Q, Wang GX, Wei NN, et al. Antipruritic effect of natural coumarin osthole through selective inhibition of thermosensitive TRPV3 channel in the skin. *Mol Pharmacol* 2018;**94**:1164−73.
32. Hu HZ, Gu Q, Wang C, Colton CK, Tang J, Kinoshita-Kawada M, et al. 2-Aminoethoxydiphenyl borate is a common activator of TRPV1, TRPV2, and TRPV3. *J Biol Chem* 2004;**279**:35741−8.
33. Gomtsyan A, Schmidt RG, Bayburt EK, Gfesser GA, Voight EA, Daanen JF, et al. Synthesis and pharmacology of (pyridin-2-yl)methanol derivatives as novel and selective transient receptor potential vanilloid 3 antagonists. *J Med Chem* 2016;**59**:4926−47.
34. Liu B, Yao J, Zhu MX, Qin F. Hysteresis of gating underlines sensitization of TRPV3 channels. *J Gen Physiol* 2011;**138**:509−20.
35. Sun SW, Wang RR, Sun XY, Fan JH, Qi H, Liu Y, et al. Identification of transient receptor potential vanilloid 3 antagonists from *Achillea alpina* L. and separation by liquid−liquid-refining extraction and high-speed counter-current chromatography. *Molecules* 2020;**25**:2025.
36. Zhou Q, Shi Y, Qi H, Liu H, Wei N, Jiang Y, et al. Identification of two natural coumarin enantiomers for selective inhibition of TRPV2 channels. *FASEB J* 2020;**34**:12338−53.
37. Gao Y, Cao E, Julius D, Cheng Y. TRPV1 structures in nanodiscs reveal mechanisms of ligand and lipid action. *Nature* 2016;**534**:347−51.
38. Klement G, Eisele L, Malinowsky D, Nolting A, Svensson M, Terp G, et al. Characterization of a ligand binding site in the human transient receptor potential ankyrin 1 pore. *Biophys J* 2013;**104**:798−806.
39. Zhai W, Zhou X, Wang H, Li W, Chen G, Sui X, et al. A novel cyclic peptide targeting LAG-3 for cancer immunotherapy by activating antigen-specific $CD8^{+}$ T cell responses. *Acta Pharm Sin B* 2020;**10**:1047−60.

40. Qu Y, Wang G, Sun X, Wang K. Inhibition of the warm temperature-activated Ca²⁺-permeable transient receptor potential vanilloid TRPV3 channel attenuates atopic dermatitis. *Mol Pharmacol* 2019;**96**:393−400.

41. Wilson SR, The L, Batia LM, Beattie K, Katibah GE, McClain SP, et al. The epithelial cell-derived atopic dermatitis cytokine TSLP activates neurons to induce itch. *Cell* 2013;**155**:285−95.

42. Sun S, Dong X. Trp channels and itch. *Semin Immunopathol* 2015;**38**: 293−307.

43. Holzer P, Izzo AA. The pharmacology of TRP channels. *Br J Pharmacol* 2014;**171**:2469−73.

44. Wilson NJ, Cole C, Milstone LM, Kiszewski AE, Hansen CD, O'Toole EA, et al. Expanding the phenotypic spectrum of olmsted syndrome. *J Invest Dermatol* 2015;**135**:2879−83.

45. Cao X, Wang H, Li Y, Lee M, Jiang L, Zhou Y, et al. Semidominant inheritance in olmsted syndrome. *J Invest Dermatol* 2016;**136**:1722−5.

46. Singh AK, McGoldrick LL, Sobolevsky AI. Structure and gating mechanism of the transient receptor potential channel TRPV3. *Nat Struct Mol Biol* 2018;**25**:805−13.

47. Pumroy RA, Samanta A, Liu Y, Hughes TE, Zhao S, Yudin Y, et al. Molecular mechanism of TRPV2 channel modulation by cannabidiol. *Elife* 2019;**8**:e48792.

48. Paulsen CE, Armache J-P, Gao Y, Cheng Y, Julius D. Structure of the TRPA1 ion channel suggests regulatory mechanisms. *Nature* 2015; **520**:511−7.

49. Liu X, Huang K, Niu Z, Mei D, Zhang B. Protective effect of isochlorogenic acid B on liver fibrosis in non-alcoholic steatohepatitis of mice. *Basic Clin Pharmacol Toxicol* 2019;**124**:144−53.

50. Liu X, Huang K, Zhang RJ, Mei D, Zhang B. Isochlorogenic acid A attenuates the progression of liver fibrosis through regulating HMGB1/TLR4/NF-kappaB signaling pathway. *Front Pharmacol* 2020;**11**:582.

51. Wu YH, Zhang XM, Hu MH, Wu XM, Zhao Y. Effect of *Laggera alata* on hepatocyte damage induced by carbon tetrachloride *in vitro* and *in vivo*. J Ethnopharmacol 2009;**126**:50−6.

52. Zheng QX, Xu ZJ, Sun XF, Gueritte F, Cesario M, Sun HD, et al. Eudesmane derivatives and other sesquiterpenes from *Laggera alata*. *J Nat Prod* 2003;**66**:1078−81.

53. Yi R, Zhang J, Sun P, Qian Y, Zhao X. Protective effects of kuding tea (*Ilex kudingcha* C. J. Tseng) polyphenols on UVB-induced skin aging in SKH1 hairless mice. *Molecules* 2019;**24**:1016.

54. Wang Q, Xiao L. Isochlorogenic acid A attenuates acute lung injury induced by LPS *via* NF-kappaB/NLRP3 signaling pathway. *Am J Transl Res* 2019;**11**:7018−26.

55. Zha RP, Xu W, Wang WY, Dong L, Wang YP. Prevention of lipopolysaccharide-induced injury by 3,5-dicaffeoylquinic acid in endothelial cells. *Acta Pharmacol Sin* 2007;**28**:1143−8.

56. Meng J, Steinhoff M. Molecular mechanisms of pruritus. *Curr Res Transl Med* 2016;**64**:203−6.

57. Werfel T, Allam JP, Biedermann T, Eyerich K, Gilles S, Guttman-Yassky E, et al. Cellular and molecular immunologic mechanisms in patients with atopic dermatitis. *J Allergy Clin Immunol* 2016;**138**: 336−49.

58. Caterina M, Pang Z. TRP channels in skin biology and pathophysiology. *Pharmaceuticals* 2016;**9**:77.

59. Shim WS, Tak MH, Lee MH, Kim M, Kim M, Koo JY, et al. TRPV1 mediates histamine-induced itching *via* the activation of phospholipase A2 and 12-lipoxygenase. *J Neurosci* 2007;**27**:2331−7.

60. Mollanazar NK, Smith PK, Yosipovitch G. Mediators of chronic pruritus in atopic dermatitis: getting the itch out?. *Clin Rev Allergy Immunol* 2015;**51**:263−92.

61. Zhang X. Targeting TRP ion channels for itch relief. *Naunyn Schmiedebergs Arch Pharmacol* 2015;**388**:389−99.

62. Nilius B, Biro T. TRPV3: a 'more than skinny' channel. *Exp Dermatol* 2013;**22**:447−52.

63. Cheng W, Yang F, Liu S, Colton CK, Wang C, Cui Y, et al. Heteromeric heat-sensitive transient receptor potential channels exhibit distinct temperature and chemical response. *J Biol Chem* 2012;**287**: 7279−88.

64. Cheng W, Yang F, Takanishi CL, Zheng J. Thermosensitive TRPV channel subunits coassemble into heteromeric channels with intermediate conductance and gating properties. *J Gen Physiol* 2007;**129**: 191−207.

65. Deng Z, Maksaev G, Rau M, Xie Z, Hu H, Fitzpatrick JAJ, et al. Gating of human TRPV3 in a lipid bilayer. *Nat Struct Mol Biol* 2020; **27**:635−44.

66. García-Martínez C, Morenilla-Palao C, Planells-Cases R, Merino JM, Ferrer-Montiel A. Identification of an aspartic residue in the P-loop of the vanilloid receptor that modulates pore properties. *J Biol Chem* 2000;**275**:32552−8.

67. Chung MK, Guler AD, Caterina MJ. Biphasic currents evoked by chemical or thermal activation of the heat-gated ion channel, TRPV3. *J Biol Chem* 2005;**280**:15928−41.

68. Luo J, Stewart R, Berdeaux R, Hu H. Tonic inhibition of TRPV3 by Mg²⁺ in mouse epidermal keratinocytes. *J Invest Dermatol* 2012;**132**: 2158−65.

Inhibition of temperature-sensitive TRPV3 channel by two natural isochlorogenic acid isomers for alleviation of dermatitis and chronic pruritus

Hang Qi[a], Yuntao Shi[b], Han Wu[a], Canyang Niu[a], Xiaoying Sun[a,c,*], KeWei Wang[a,c,*]

[a]*Department of Pharmacology, School of Pharmacy, Qingdao University, Qingdao 266021, China*

[b]*State Key Laboratory of Natural and Biomimetic Drugs, School of Pharmaceutical Sciences, Peking University, Beijing 100191, China*

[c]*Institue of Innovative Drugs, Qingdao University, Qingdao 266021, China*

Received 22 April 2021; received in revised form 13 July 2021; accepted 30 July 2021

[*]Corresponding authors.

E-mail addresses: xiaoyingsun@qdu.edu.cn (Xiaoying Sun), wangkw@qdu.edu.cn (KeWei Wang).

Table S1 The docking scores of IAA and IAB in mTRPV3.

| Pocket	Pocket description	Glide score of IAA	Glide score of IAB
A	CBD binding to TRPV2 pocket and A967079 binding to TRPA1 pocket	−8.9	−9.1
B	Capsaicin binding to TRPV1 pocket	−7.3	−6.5
C	2-APB binding to TRPV3 pocket	−7.2	−5.2
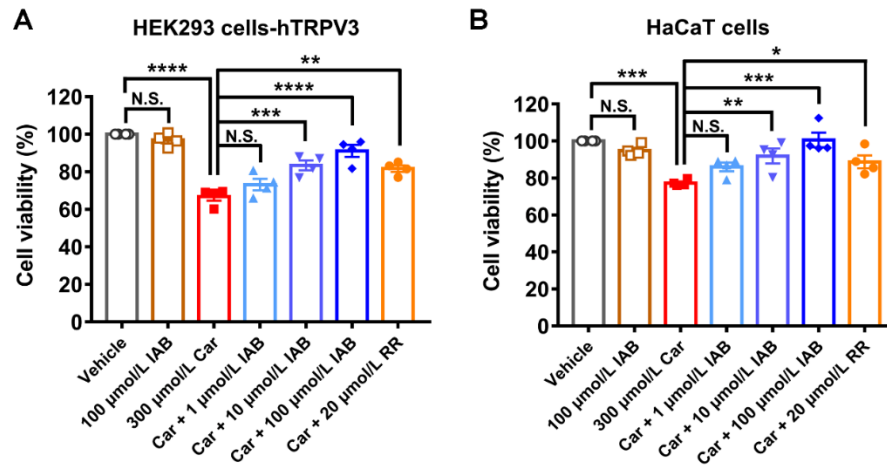
Figure S1 IAB reversed the proliferation inhibition of HEK293 cells expressing TRPV3 or HaCaT cells induced by overactiving TRPV3. Cell viability of HEK293 cells expressing hTRPV3 (A) or HaCaT cells (B) after treatment with different TRPV3 modulators for 24 h in MTT assay ($n = 4$; $*P < 0.05$, $**P < 0.01$, $***P < 0.001$, $****P < 0.0001$; N.S., no significance; by one-way ANOVA, followed by the Dunnet's test). Data are presented as the mean ± SEM.

Figure S2 Residue sequence alignment of pore helix and upper portion of S6 between mouse TRPV3 and human TRPV3.
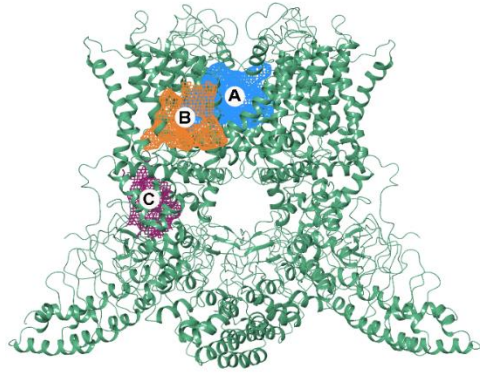
Figure S3 Illustration of three docking pockets in meshes in three different colors in mTRPV3. Pocket A in blue for the isomers IAA and IAB binding, correlating to the binding site for TRPV2 agonist CBD and TRPA1 inhibitor A967079. Pocket B in orange consisted of S4 and S4–S5 linker, corresponding to the capsaicin binding site in TRPV1. Pocket C in purple showing the 2-APB binding site in mTRPV3.
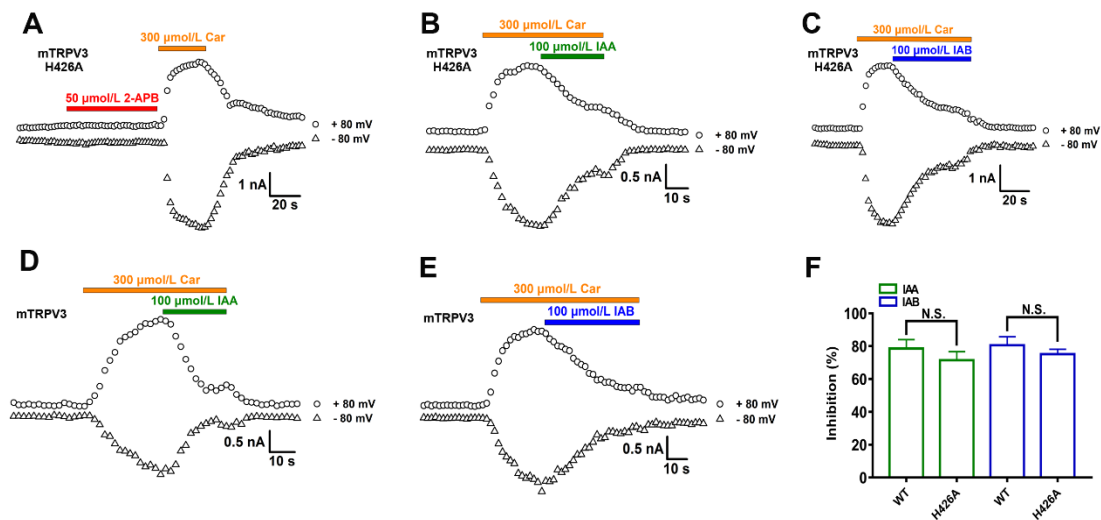
Figure S4 The residue H426 in mTRPV3 is critical for the binding of 2-APB, but not for IAA and IAB. (A) A representative current trace of mTRPV3 H426A mutant in response to carvacrol (300 μmol/L) or 2-APB (50 μmol/L). (B and C) Representative current traces for inhibition of carvacrol-activated mTRPV3 H426A mutant channels by IAA or IAB. (D and E) Representative current traces for inhibition of WT mTRPV3 channels by IAA or IAB. (F) Summary for current inhibition of WT mTRPV3 or H426A mutant channel by 100 µmol/L IAA and IAB ($n = 4$). Data are expressed as the mean ± SEM. N.S., no significance, by unpaired t test.